Optik 168 (2018) 956–962

Contents lists available at ScienceDirect

Optik

journal homepage: www.elsevier.de/ijleo

Original research article

Scintillation properties of SrF_2 translucent ceramics and crystal

Takumi Kato [a,*], Naoki Kawano [a], Go Okada [a], Noriaki Kawaguchi [a], Kentaro Fukuda [b], Takayuki Yanagida [a]

[a] Graduate School of Materials Science, Nara Institute of Science and Technology (NAIST), 8916-5 Takayama-cho, Ikoma-shi, Nara 630-0192, Japan
[b] Tokuyama Corp., 1-1 Mikage-cho, Shunan-shi, Yamaguchi 745-8648, Japan

ARTICLE INFO

Article history:
Received 12 March 2018
Accepted 11 April 2018

Keywords:
Translucent ceramics
SrF_2
Scintillator

ABSTRACT

We have developed SrF_2 translucent ceramic by using the spark plasma sintering (SPS) method, and investigated scintillation properties and thermally stimulated luminescence (TSL) glow curves, in comparison with a SrF_2 crystal. Both of the samples showed scintillation with emission peaks at 300 nm under X-ray irradiation. Based on the scintillation decay times measured, the origin of emission at 300 nm was attributed to self-trapped excitation. The scintillation light yield of the SrF_2 translucent ceramic was evaluated to be about 8900 photons/MeV under ^{57}Co γ-rays. In addition, the afterglow level of the translucent ceramic was lower than that of the crystal.

1. Introduction

Inorganic scintillators are one of the luminescent materials which absorbs and instantly converts the energy of incident ionizing radiation to thousands of ultraviolet/visible photons. An attention in new scintillators materials is promoted by an increasing number of new applications such as medical [1], security [2], oil-logging [3], environmental monitoring [4], astro [5] and particle physics [6]. The most prospective scintillators are bromides and iodides doped with Ce^{3+} and Eu^{2+} ions such as strontium iodide doped with Eu^{2+} ions (SrI_2:Eu) and lanthanum bromide doped with Ce^{3+} ions ($LaBr_3$:Ce). These crystals have a high light yield (100,000 photons/MeV for SrI_2:Eu), good energy resolution and short decay times [7]. Disadvantages of these scintillators are to have a high hygroscopicity. In addition, it was reported that SrI_2:Eu had temperature instability of the light yield [8]. On the other hand, alkaline earth fluorides have a low hygroscopicity, low phonon energy and high radiation resistance [9,10]. For example, Barium fluoride (BaF_2) single crystals are known as a potential scintillator material. In the 1970s, Farukhi and Swinehart have first reported scintillation emissions of BaF_2 crystals due to auger-free luminescence (AFL) and self-trapped excitation (STE), which appeared around 190–220 and 310 nm, respectively [11]. In particular, BaF_2 has considerably large effective atomic number, so it has a great advantage to use for γ-ray detections. Calcium fluoride (CaF_2) single crystals are known to show a scintillation emission due to STE at 270 nm [12]. Moreover, it has a large band gap energy and relatively high light yield (13,000 photons/MeV) [13], and CaF_2 has been investigated for potential as the scintillator in astrophysics [14].

* Corresponding author.
E-mail address: kato.takumi.ki5@ms.naist.jp (T. Kato).

https://doi.org/10.1016/j.ijleo.2018.04.082
0030-4026/

Today, almost all the scintillators used in practice are bulk single crystals because they have the excellent properties such as high transparency, high light yield and high detection efficiency due to the volume. However, recent studies [16–19] have opened up a new possibility of using transparent ceramics as scintillators material thanks to an achievement of improved synthesis technologies developed with an advancement of the laser field [20]. Compared with the single crystals, the ceramics have many advantages such as the mechanical strength, flexible geometric shape to be prepared and cost effectiveness. Furthermore, they have also been found to show an equivalent or even superior performance as a scintillator compared with the single crystal form [16–19]. These studies have been done on the oxide materials, and we have started to investigate fluoride materials with transparent or translucent form on scintillation properties. Up to now, our groups have developed and evaluated CaF_2 and BaF_2 transparent ceramics for scintillator applications [21,22].

In this study, to extend our previous research, we developed the undoped SrF_2 translucent ceramic by using the spark plasma sintering (SPS) method and characterized scintillation properties in comparison with a SrF_2 crystal prepared by the simple solidification method. Furthermore, we measured the thermally stimulated luminescence (TSL) glow curve in order to study relatively shallow trapping centers. Scintillation properties of SrF_2 single crystals have already been investigated, and the light yield was estimated about 18,000 photons/MeV under ^{137}Cs γ-ray irradiation [23]. However, no report can be found about scintillation properties of SrF_2 translucent ceramics.

2. Experiment

SrF_2 translucent ceramic sample was synthesized by the SPS method using Sinter Land LabX-100 as follows. First, SrF_2 powder (1.0 g) of a reagent grade was loaded in a graphite die and sealed with two graphite punches, and a graphite assembly was loaded to the furnace to sinter. The temperature during the sintering was controlled as described in the following sequence: the temperature was increased from 20 °C to 890 °C at a rate of 10 °C/min and held for 10 min while applying a pressure of 10 MPa, and then the temperature was increased to 1080 °C at the rate of 10 °C/min and held for 20 min while applying a pressure of 100 MPa in vacuum. The SrF_2 crystal sample was synthesized by the simple solidification method. The SrF_2 raw powders were put into a carbon crucible. The crucible were set in the stainless chamber and were enclosed by the carbon resist heater. Most parts of hot zone are made of high purity carbon. After the setting of crucibles and hot zone, the chamber was evacuated up to 8×10^{-4} Pa. Then, the crucible was heated up to 400 °C and kept for about 20 min at this temperature in order to remove oxygen traces caused by moisture of raw materials and adsorbates on the chamber surface. After the baking, the chamber was filled with Ar gas until ambient pressure. Then, the crucible was heated to no less than the melting point of SrF_2 and kept for 30 min. The translucent ceramic and crystal samples were synthesized by using the same SrF_2 powders provided by Tokuyama Corp. Backscattered electron image of the ceramic sample was obtained by using scanning electron microscope (SEM; Hitachi TM3030). SEM images were observed on the polished surface. Optical in-line transmittance was evaluated by a spectrometer (V670, JASCO) over the spectral range of 190–2700 nm with 1 nm intervals.

The scintillation spectra from 250 to 700 nm were measured using a setup [19]. A CCD-based spectrometer (ANDOR DU920-BU2NC) was used to measure the emission spectrum. The excitation source was an X-ray generator which was supplied by a bias voltage and tube current of 80 kV and 1.2 mA, respectively. An optical fiber was used to guide the scintillation photons to the spectrometer. In order to evaluate X-ray induced scintillation decay times of STE, we used an afterglow characterization system equipped with a pulse X-ray tube [24]. Furthermore, to investigate the amount of shallow defects qualitatively, afterglow profiles by X-ray irradiation was measured using also the afterglow characterization system.

The pulse height spectra with ^{57}Co γ-ray exposure were investigated to grasp scintillation light yield. We mounted a sample piece on the window of PMT (R877-100, Hamamatsu) with a silicon grease (6262A, OKEN), and the sample was covered by several layers of Teflon reflectors to guide scintillation photons to the photoelectric converter of the PMT. The bias voltage of −600 V was applied to the PMT by a DC power supply (ORTEC 113), and the electrical signal output from the anode of the PMT was amplified by a preamplifier (ORTEC 113). Furthermore, the amplified signal was processed by a shaping amplifier (ORTEC 572) with 1.0 μs shaping time to obtain the light output, which was then processed by a multichannel analyzer (Amptek Pocket MCA 8000A) to convert analog signals to digital. Finally, the pulse height spectrum was collected in the computer.

In order to characterize relatively shallow trapping centers, we have measured a TSL glow curve using a Nanogray TL-2000 [25] after X-ray irradiations with 10 Gy. The heating rate used for all the TSL measurements was fixed to 1 °C/s, and the sample was heated from 50 to 490 °C to measure the glow curve.

3. Results and discussion

3.1. Sample

Fig. 1 shows the synthesized SrF_2 translucent ceramic and crystal samples. The thickness of the translucent ceramic and crystal samples were 0.61 and 0.68 mm, respectively. It can be confirmed that the stripe patterns on the back of samples are clearly seen through. Fig. 2 illustrates SEM image of ceramic sample. From the SEM images, it can be confirmed that the ceramic samples were highly densified and properly sintered. Fig. 3 shows transmittance spectra of the SrF_2 translucent

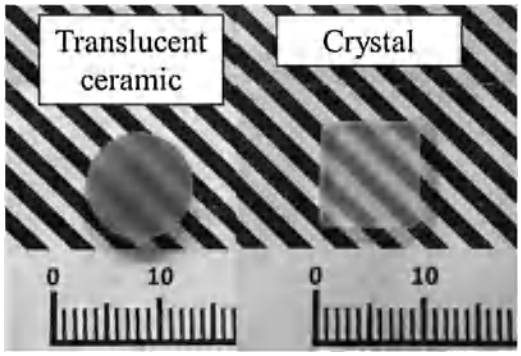

Fig. 1. Synthesized SrF_2 translucent ceramic and crystal samples.

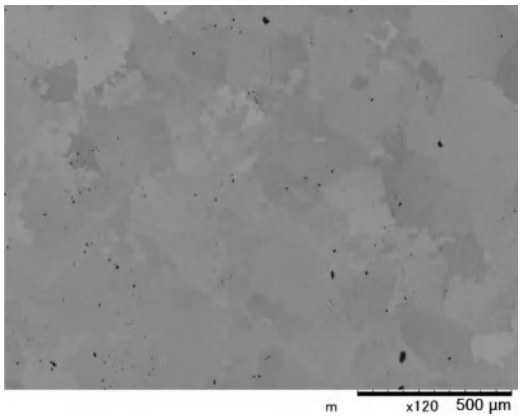

Fig. 2. SEM image of the SrF_2 translucent ceramic sample.

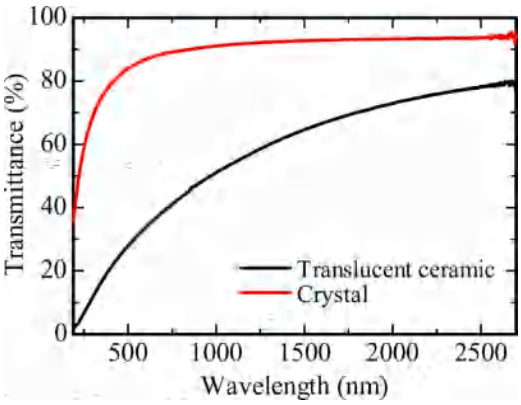

Fig. 3. Transmittance spectra of the SrF_2 translucent ceramic and crystal samples.

ceramic and crystal samples. The transmittance of the translucent ceramic was lower than that of the crystal in the measured spectral range.

3.2. Scintillation properties

X-ray induced scintillation spectra of the SrF_2 translucent ceramic and crystal samples are presented in Fig. 4. Both of the samples showed an emission peak around 300 nm and had similar spectral shapes. The slight difference of the emission peak wavelength was ascribed to the difference of the transmittance in the ultra violet range. Similar emission peak around 300 nm was also reported by earlier works [26,27], in which the origin of this mission was ascribed to STE. Fig. 5 shows the X-ray induced scintillation decay time profiles of the SrF_2 translucent ceramic and crystal samples. The decay curves were approximated by a sum of two exponential functions. The obtained decay time constants were 310 and 1113 ns for the

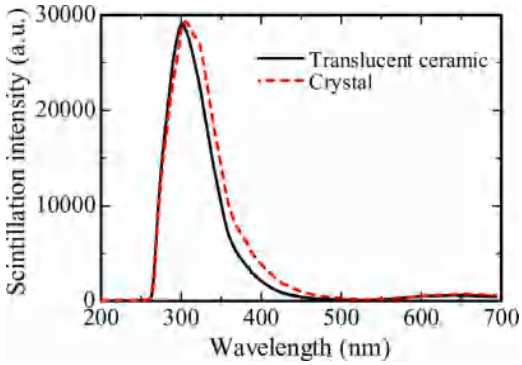

Fig. 4. X-ray induced scintillation spectra of the SrF_2 translucent ceramic and the crystal samples.

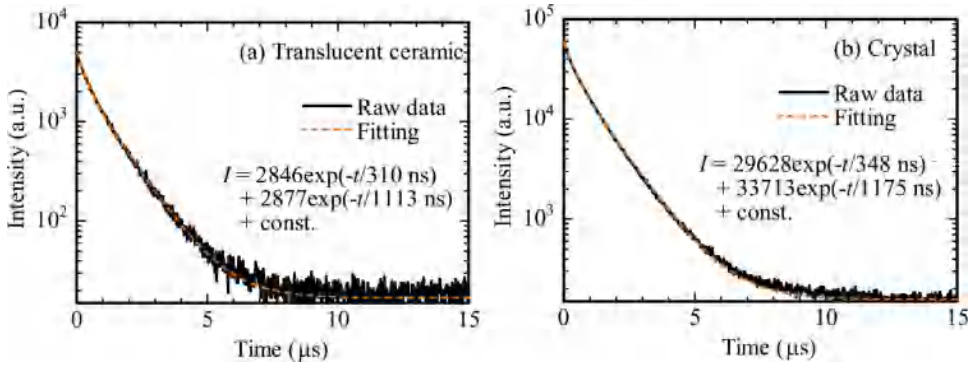

Fig. 5. X-ray induced scintillation decay time profiles of the SrF_2 (a) translucent ceramic and (b) crystal samples.

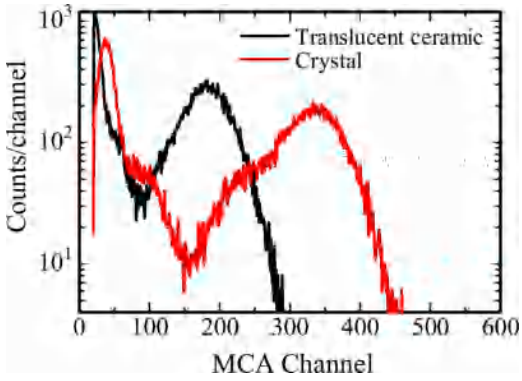

Fig. 6. Pulse height spectra of the SrF_2 translucent ceramic and crystal samples under ^{57}Co γ-ray irradiation.

translucent ceramic sample, 348 and 1175 ns for the crystal sample. These components are consistent with the previously reported values [28–30], so the origins of these components are attributed to STE.

Fig. 6 demonstrates pulse height spectra of the SrF_2 translucent ceramic and crystal samples under ^{57}Co γ-ray irradiation. The light yields of the translucent ceramic and crystal were estimated to 8900 and 16,400 photons/MeV, respectively. The light yields were derived as relative values to that of conventional NaI:Tl crystal scintillator [31]. Although the light yield of the crystal was close to the past observation [23], the light yield of the ceramic sample was smaller than that of the crystal sample. This can arise from a trapping of excited electrons in something of defects and/or impurity ions in the translucent ceramic sample or simply due to the low optical transmittance.

Fig. 7 shows afterglow profiles after an X-ray irradiation with a pulse duration of 2 ms. Afterglow levels of translucent ceramic and crystal are 0.0079 and 0.0153%, respectively. From this result, it can be said that afterglow levels of translucent ceramics are improved in comparison with the one of crystal although many grain boundaries are created in ceramics. In this evaluation, afterglow levels (A) are represented $A\ (\%) = 100 \times (I_2 - I_0)/(I_1 - I_0)$ where I_0–I_2 denote the averaged background signal, the averaged signal intensity during X-ray irradiation and signal intensity at 20 ms after the X-ray irradiation,

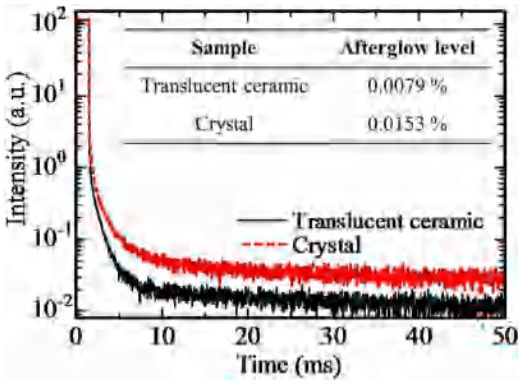

Fig. 7. Afterglow profiles of the SrF_2 translucent ceramic and crystal samples after an X-ray irradiation with a pulse duration of 2 ms.

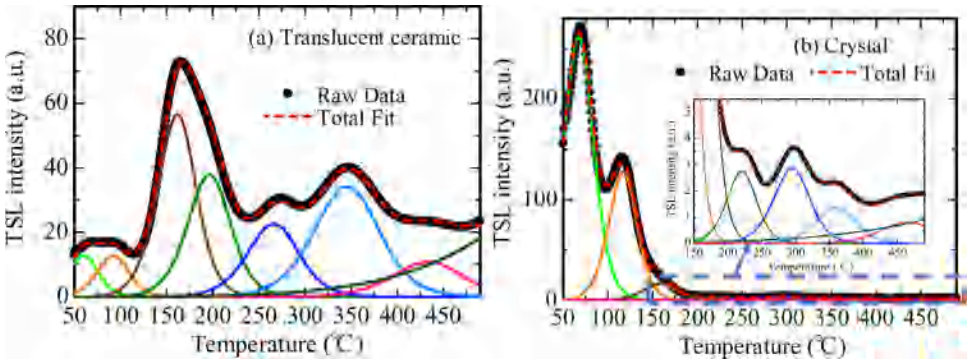

Fig. 8. TSL glow curves with GCD function of (a) translucent ceramic and (b) crystal. The inset in Fig. 8(b) extends 150–490 °C range.

Table 1
The parameters of the GCD functions for the SrF_2 (a) translucent ceramic and (b) crystal samples.

(a)	Peak 1	Peak 2	Peak 3	Peak 4	Peak 5	Peak 6	Peak 7
T_m (°C)	60	92	161	196	266	345	433
I_m (a.u.)	16.5	16.5	73.2	49	29	44	14
E (ev)	0.73	0.82	0.97	1.01	1.10	1.15	1.40
(b)	Peak 1	Peak 2	Peak 3	Peak 4	Peak 5	Peak 6	Peak 7
T_m (°C)	67	117	158	221	295	360	465
I_m (a.u.)	339	212	21	3.55	3.7	1.75	1.05
E (ev)	0.75	1.05	1.1	1.2	1.3	1.48	1.5

respectively. We referred the formula from the evaluation manner of NIHON KESSHO KOGAKU CO., LTD. which is one of the well-known manufactures of scintillation detectors for medical and security applications. In general, the ceramic sample has more defects than the crystal; however, the afterglow level of the translucent ceramic is smaller than that of the crystal. We thought that the present result may be explained by the following two possbilities: (1) In the crystal sample, most trapping centers have low activation energy so the trapping and detrapping processes can be observed as a slow emission component. In this case, TSL glow peaks can be observed at low temperatures below room temperature. (2) In the translucent ceramic, the defects are acting as quenching centers at room temperature.

3.3. TSL glow curve

Fig. 8 shows TSL glow curves of (a) translucent ceramic and (b) crystal samples measured after the samples were irradiated with an X-ray dose of 1 Gy. The glow curves were decomposed by glow curve deconvolution (GCD) functions described in [32]. The parameters obtained by the deconvolutions were summarized in Table 1. The free parameters of the GCD functions are the maximum peak temperature (T_m), the maximum peak intensity (I_m) and the activation energy (E). The glow curves were best-fitted by seven GCD functions, and the translucent ceramic showed glow peaks about 36, 92, 158, 193, 259, 339 and 433 °C while the crystal showed glow peaks about 58, 114, 149, 213, 291, 361 and 455 °C. A number of peaks was the same between the translucent ceramic and crystal; however, the peak temperatures were slightly difference. In terms of shallow

trapping centers, the crystal showed higher intensities than translucent ceramic. Actually, TSL intensity of the crystal from 50 to 150 °C was around twice as large as that of the ceramic, and it coincided with the afterglow levels of these samples. From these results, in the above discussion about afterglow levels, we considered that the reason (1) was more reasonable than the reason (2). In addition, the total intensities of these samples over the whole temperature range were almost the same, and it meant that numbers of trapped carriers were almost the same. Thus the lower scintillation light yield of the ceramic would be blamed for the low optical transmittance.

4. Conclusions

We have developed SrF_2 translucent ceramic by the SPS method and then investigated the scintillation properties and TSL glow curves, in comparison with SrF_2 crystal. The emission due to the STE was detected for the translucent ceramic sample as well as the crystal sample. In addition, the absolute light yield of the translucent ceramic sample was approximately 8900 photons/MeV. Although the light yield of translucent ceramic is inferior to the crystal in this time, the light yield would be improved when the optical transmittance is enhanced by that the synthesis methods and conditions are optimized as same as the cases of transparent ceramic garnet scintillators. The afterglow level of translucent ceramic was better than that of the crystal. These results consist of the results in TSL intensities of translucent ceramic and crystal.

Acknowledgements

This work was supported by Grant-in-Aid for Scientific Research (A) (17H01375), Grant-in-Aid for Young Scientists (B) (17K14911) and Grant-in-Aid for Research Activity Start-up (16H06983) from the Ministry of Education, Culture, Sports, Science and Technology of the Japanese government (MEXT) as well as A-STEP from Japan Science and Technology Agency (JST). The Cooperative Research Project of Research Institute of Electronics, Shizuoka University, Mazda Foundation, Konica Minolta Science and Technology Foundation, Taisei Foundation, Terumo Foundation for Life Sciences and Arts, Izumi Science and Technology Foundation, SEI Group CSR Foundation, The Iwatani Naoji Foundation, NAIST Foundation and TEPCO Memorial Foundation are also acknowledged.

References

[1] C.W.E. Van Eijk, Inorganic scintillators in medical imaging detectors, Nucl. Instrum. Methods Phys. Res. Sect. A: Accel. Spectrom. Detect. Assoc. Equip. 509 (2003) 17–25.
[2] J.M. Hall, S. Asztalos, P. Biltoft, J. Church, M.A. Descalle, T. Luu, D. Manatt, G. Mauger, E. Norman, D. Petersen, J. Pruet, S. Prussin, D. Slaughter, The nuclear car wash: neutron interrogation of cargo containers to detect hidden SNM, Nucl. Instrum. Methods Phys. Res. Sect. B Beam Interact. Mater. Atoms. 261 (2007) 337–340.
[3] T. Yanagida, Y. Fujimoto, S. Kurosawa, K. Kamada, H. Takahashi, Y. Fukazawa, M. Nikl, V. Chani, Temperature dependence of scintillation properties of bright oxide scintillators for well-logging, Jpn. J. Appl. Phys. 52 (2013) 076401.
[4] K. Watanabe, T. Yanagida, K. Fukuda, A. Koike, T. Aoki, A. Uritani, Portable neutron detector using Ce:$LiCaAlF_6$ scintillator, Sens. Mater. 27 (2015) 269–275.
[5] M. Kokubun, K. Abe, Y. Ezoe, Y. Fukazawa, S. Hong, H. Inoue, T. Itoh, T. Kamae, D. Kasama, M. Kawaharada, N. Kawano, K. Kawashima, S. Kawasoe, Y. Kobayashi, J. Kotoku, M. Kouda, A. Kubota, G.M. Madejski, K. Makishima, T. Mitani, H. Miyasaka, R. Miyawaki, K. Mori, M. Mori, T. Murakami, M.M. Murashima, K. Nakazawa, H. Niko, M. Nomachi, M. Ohno, Y. Okada, K. Oonuki, G. Sato, M. Suzuki, H. Takahashi, I. Takahashi, T. Takahashi, K. Tamura, T. Tanaka, M. Tashiro, Y. Terada, S. Tominaga, S. Watanabe, K. Yamaoka, T. Yanagida, D. Yonetoku, Development of the HXD-II wide-band all-sky monitor onboard Astro-E2, IEEE Trans. Nucl. Sci. 52 (2005) 2765–2772.
[6] T. Ito, T. Yanagida, M. Sato, M. Kokubun, T. Takashima, S. Hirakuri, R. Miyawaki, H. Takahashi, K. Makishima, T. Tanaka, K. Nakazawa, T. Takahashi, T. Honda, A1-dimensional γ-ray position sensor based on GSO:Ce scintillators coupled to a Si strip detector, Nucl. Instrum. Methods A 579 (2007) 239–242.
[7] T. Yanagida, M. Koshimizu, G. Okada, T. Kojima, J. Osada, N. Kawaguchi, Comparative study of nondoped and Eu-doped SrI_2 scintillator, Opt. Mater. 61 (2016) 119–124.
[8] M. Alekhin, Jd. Haas, K. Kramer, P. Dorenbos, Scintillation properties of and self absorption in SrI_2:Eu^{2+}, IEEE Trans. Nucl. Sci. 58 (2011) 2519–2527.
[9] R. Shendrik, E.A. Radzhabov, A.I. Nepomnyashchikh, Scintillation properties of pure and Ce^{3+}-doped SrF_2 crystals, Radiat. Meas. 56 (2013) 58–61.
[10] M. Yagoub, H. Swart, L. Noto, P. Bergman, E. Coetsee, Surface characterization and photoluminescence properties of Ce^{3+}, Eu co-doped SrF_2 nanophosphor, Materials 8 (2015) 2361–2375.
[11] M.R. Farukhi, C.F. Swinehart, Barium fluoride as a gamma ray and charged particle detector, Nucl. Sci. 18 (1971) 200–204.
[12] L.P. Cramer, T.D. Cumby, J.A. Leraas, S.C. Langford, J.T. Dickinson, Effect ofsurface treatments on self-trapped exciton luminescence in single-crystalCaF_2, J. Appl. Phys. 97 (2005) 1–6.
[13] R.A. Heaton, C.C. Lin, Electronic energy-band structure of the calcium fluridecrystal, Phys. Rev. B 22 (1980) 3629.
[14] Y. Shimizu, M. Minowa, W. Suganuma, Y. Inoue, Dark matter searchexperiment with CaF_2:Eu scintillator at Kamioka observatory, Phys. Lett. B633 (2006) 195–200.
[16] T. Yanagida, H. Takahashi, T. Ito, D. Kasama, T. Enoto, M. Sato, S. Hirakuri, M. Kokubun, K. Makishima, T. Yanagitani, H. Yagi, T. Shigeta, T. Ito, Evaluation of properties of YAG (Ce) ceramic scintillators, IEEE Nucl. Trans. Sci. 52 (2005) 1836–1841.
[17] T. Yanagida, Y. Fujimoto, Y. Yokota, K. Kamada, S. Yanagida, A. Yoshikawa, H. Yagi, T. Yanagitani, Comparative study of transparent ceramic and single crystal Ce doped LuAG scintillators, Radiat. Meas. 46 (2011) 1503–1505.
[18] T. Yanagida, Y. Fujimoto, K. Kamada, D. Totsuka, H. Yagi, T. Yanagitani, Y. Futami, S. Yanagida, S. Kurosawa, Y. Yokota, A. Yoshikawa, M. Nikl, Scintillation properties of transparent ceramic Pr:LuAG for different Pr concentration, IEEE Trans. Nucl. Sci. 59 (2012) 2146–2151.
[19] T. Yanagida, K. Kamada, Y. Fujimoto, H. Yagi, T. Yanagitani, Comparative studyof ceramic and single crystal Ce:GAGG scintillator, Opt. Mater. 35 (2013) 2480–2485.
[20] J. Lu, M. Prabhu, J. Song, C. Li, J. Xu, K. Ueda, A.A. Kaminskii, H. Yagi, T. Yanagitani, Optical properties and highly efficient laser oscillation of Nd:YAG ceramics, Appl. Phys. B 71 (2000) 469–473.
[21] T. Kato, G. Okada, K. Fukuda, T. Yanagida, Development of BaF_2 transparent ceramics and evaluation of the scintillation properties, Radiat. Meas. 107 (2017) 140–145.

[22] F. Nakamura, T. Kato, G. Okada, N. Kawaguchi, K. Fukuda, T. Yanagida, Scintillation and dosimeter properties of CaF_2 translucent ceramic produced by SPS, J. Eur. Ceram. Soc. 37 (2017) 1707–1711.
[23] R. Shendrik, E.A. Radzhabov, A.I. Nepomnyashchikh, Scintillation properties of SrF_2 and SrF_2-Ce^{3+} crystals, Tech. Phys. Lett. 7 (2013) 587–590.
[24] T. Yanagida, Y. Fujimoto, T. Ito, K. Uchiyama, K. Mori, Development of X-ray-induced afterglow characterization system, Appl. Phys. Express 7 (2014) 8–11.
[25] T. Yanagida, Y. Fujimoto, N. Kawaguchi, S. Yanagida, Dosimeter properties of AlN, J. Ceram. Soc. Jpn. 121 (2013) 988–991.
[26] R.T. Williams, M.N. Kabler, Time-resolved spectroscopy of self-trapped excitations in fluorite crystals, Phys. Rev. B 14 (1976) 725–740.
[27] R. Shendrik, E.A. Radzhabov, A.I. Nepomnyashchikh, Scintillation properties of pure and Ce^{3+}-doped SrF_2 crystals, Radiat. Meas. 56 (2013) 58–61.
[28] R. Lindner, R.T. Williams, M. Reichling, Time-dependent luminescence of self-trapped excitons in alkaline-earth fluorides excited by femtosecond laser pulses, Phys. Rev. B 63 (2001) 075110.
[29] R. Shendrik, E.A. Radzhabov, Absolute light yield measurements on SrF_2 and BaF_2 doped with rare earth ions, J. Cl. Files 6 (2012) 1–5.
[30] N. Fedorov, A. Belsky, E. Constant, D. Descamps, P. Martin, A.N. Vasil'ev, Quenching of excitonic luminescence of alkaline earth fluorides excited by VUV harmonics of femtosecond laser, J. Lumin. 129 (2009) 1813–1816.
[31] R. Hofstadter, Phys. Rev. 74 (1948) 100–101.
[32] G. Kitis, J.M. Gomez-Ros, J.W.N. Tuyn, Thermoluminescence glow-curve deconvolution functions for first, second and general orders of kinetics, J. Phys. D: Appl. Phys. 31 (1998) 2636–2641.